

Comparison of Triple Frequency GNSS Carrier Phase and Pseudorange noise using various satellite constellations.

Gethin Wyn ROBERTS, Faroe Islands
Craig M. HANCOCK, X. TANG, China

Key words: GNSS, carrier phase, pseudorange, observable noise

SUMMARY

The first Global Positioning System (GPS) satellite was launched in 1978, and today there are 4 Global Navigation Satellite Systems (GNSS), with a further 7 Space Based Augmentation Systems (SBAS) and Regional Navigation Satellite Systems (RNSS) transmitting data. Further to this, these systems consist of three basic types of satellite orbits, namely Mid Earth Orbiting (MEO), Geosynchronous Orbits (GEO) and Inclined Geosynchronous Orbits (IGSO) operating at different altitudes. It is now possible to see and take measurements up to almost 50 satellites at any instant in some parts of the world, and typically in the region of 30 in most parts of the world. Originally, GPS transmitted data on two carrier frequencies, namely L1 and L2. Today's GPS satellites transmit a variety of contemporary and original code data on three carrier frequencies; L1, L2 and L5. Similarly, other GNSS transmit on three or more carrier frequencies.

This paper looks at the quality of the data from GPS, BeiDou, Galileo, GLONASS and QZSS, looking at the different satellite constellations used, as well as the different frequencies and also the historical satellite systems such as the various GPS blocks. The approaches used in this paper, are those also used for cycle slip detection. These are namely the range residual (code-carrier), and the Ionospheric Residual. In this paper, however, the noise of these combinations is investigated and compared, illustrating the expected measurement precisions from the different types of satellites, and their comparisons.

Comparison of Triple Frequency GNSS Carrier Phase and Pseudorange noise using various satellite constellations.
(9452)

Gethin Wyn Roberts (Faroe Islands), Craig Hancock and X Tang (China, PR)

FIG Congress 2018

Embracing our smart world where the continents connect: enhancing the geospatial maturity of societies
Istanbul, Turkey, May 6–11, 2018

Comparison of Triple Frequency GNSS Carrier Phase and Pseudorange noise using various satellite constellations.

Gethin Wyn ROBERTS, Faroe Islands, Craig HANCOCK, China

1. INTRODUCTION

The first Global Positioning System (GPS) satellite was launched in 1978, transmitting pseudorange codes on L1 (1575.42 MHz) and L2 (1227.60 MHz) carrier frequencies. Today, there are four Global Navigation Satellite Systems (GNSS) transmitting various codes on various carrier frequencies. These are the USA's GPS, Russia's GLONASS, Europe's Galileo and China's BeiDou. Most of the carrier phase and pseudorange data are available using civilian GNSS receivers. In addition to this, GPS and subsequent GNSS such as the Russian GLONASS and European Galileo use Mid Earth Orbiting (MEO) satellites to transmit the data. These typically orbit at altitudes of 20,200km (GPS), 19,100km (GLONASS) and 23,222km (Galileo). However, the regional Japanese Quazi Zenith Satellite System incorporates Inclined Geosynchronous Orbits (IGSO) with satellites at perigee altitude of about 32,000 km and apogee altitude about 40,000 km. BeiDou incorporates three different types of orbits, these being MEO at around 27,878km, IGSO and Geosynchronous (GEO) orbits both at around 42,164km.

Further to this, various GNSS, in particular the older systems such as GPS and GLONASS, have successive generations of satellites. GPS, for example, began its evolution through launching a tranche of 11 Block I satellites between 1978 and 1985. Following this, 28 Block II and IIA satellites were launched, followed by 20 Block IIR and a further eight Block IIR-M satellites. The latest tranche of satellites to be launched are Block IIF, initially launched in May 2010, these satellites include a third civil frequency, L5 (1176.45 MHz). The final of the 12 Block IIF satellites was launched in February 2016. The new tranche of 10 Block IIIA satellites was initially planned to start launching in 2014, but significant delays have pushed the scheduled launch back to May 2018. The final Block IIIA satellite is planned to be launched in 2023. Improvements in signal quality as well as reliability of the satellites are seen through the generations, as well as the introduction of new signals, such as L1C, L2C, L5 carrier and codes, as well as M-codes, on top of the existing L1-C/A code and the P code on both L1 and L2. Improvements are also seen in boosting the transmitting power.

This paper investigates the use of two approaches to analyse the relative noise in the various carrier phase and pseudorange observable for GPS, BeiDou, Galileo, GLONASS and QZSS. In addition, results are presented for GPS Block IIA, Block IIR, Block IIRM and Block IIF satellites.

Comparison of Triple Frequency GNSS Carrier Phase and Pseudorange noise using various satellite constellations.
(9452)

Gethin Wyn Roberts (Faroe Islands), Craig Hancock and X Tang (China, PR)

FIG Congress 2018

Embracing our smart world where the continents connect: enhancing the geospatial maturity of societies
Istanbul, Turkey, May 6–11, 2018

2. OBSERVABLES

Two approaches are used in this paper to analyse the relative noise in the observables. These are called the range residual, and the ionospheric residual. Both techniques can also be used to detect cycle slips [Roberts, 2017].

2.1 Range Residual

The range residual is simply the change from one epoch to the next in the difference in the range calculated using the pseudorange and the range calculated by the carrier phase on a specific frequency. The pseudorange values are scaled using the wavelength to an equivalent range in units of the carrier's cycles rather than metres. Equation 1 illustrates the range residual between the pseudorange ρ on a specific carrier frequency and the carrier phase observable ϕ , using the wavelength λ of the carrier to scale the pseudorange. The values of these observables are compared between epochs i and $i-1$.

$$RR = \frac{(\rho_{(i)} - \rho_{(i-1)})}{\lambda} - (\phi_{(i)} - \phi_{(i-1)}) \quad \text{Eq. 1}$$

Two adjacent epochs are used as in equation 1, as then the integer ambiguity value, as well as the ionospheric and tropospheric errors, and satellite and receiver clock errors are the same, or negligibly different at such small (<1s) epoch intervals, at epochs i and $i-1$. Therefore, these are all cancelled out in Equation 1, and the resulting range residual is the measurement receiver and observable noise. The pseudorange observable will be significantly noisier than the carrier phase observable, therefore this method is a good way to calculate the measurement noise for the pseudoranges.

2.2 Ionospheric Residual

If the carrier waves travelled only through a vacuum, then a phase observation from a specific satellite to a specific GNSS receiver could be scaled and converted to an equivalent phase measurement on another frequency using the frequencies of the carrier waves [Roberts, 2017]. However, as the signal passes through the ionosphere, systematic errors which are frequency dependent are introduced, so it is not possible to directly convert from one carrier phase value to another for a specific range measurement. The error is known as the ionospheric residual, and this will change slowly over time as the satellite passes overhead and the ionosphere being passed through changes, and also as the ionosphere slowly changes its characteristics over time, mainly due to the sun's activities, or as the user changes location. The electromagnetic characteristics of the ionosphere itself will also change over time [Goad, 1986]. The Ionospheric Residual value is defined in Equation 2 [Roberts, 1997].

$$IR_a = \phi_a - \phi_b \cdot \left(\frac{f_a}{f_b}\right) + \varepsilon \quad \text{Eq. 2}$$

Comparison of Triple Frequency GNSS Carrier Phase and Pseudorange noise using various satellite constellations. (9452)

Gethin Wyn Roberts (Faroe Islands), Craig Hancock and X Tang (China, PR)

FIG Congress 2018

Embracing our smart world where the continents connect: enhancing the geospatial maturity of societies
Istanbul, Turkey, May 6–11, 2018

ϕ_a and ϕ_b are the carrier phase observables from the same satellite at the same epoch, but at two frequencies, such as L1 and L2, or L2 and L5, or B1 and B3. f_a and f_b are the corresponding frequencies for these carrier phase values, and ε represents the errors due to the ionosphere, troposphere, receiver noise and integer ambiguity. The ionospheric residual will change slowly over time, of the order of 1 cycle per minute. Equation 3 illustrates the comparison of the ionospheric residual at epochs i and $i-1$. Equation 3 therefore eliminates other error sources or unknowns ε , as this value will change very slightly from one epoch to the next, when considering small epoch intervals such as $<1s$. When considering data with no cycle slips, then the ionospheric residual values at subsequent epochs will be very similar in value, and change slowly, but will also give an indication of the receiver's carrier phase noise, which can be related to other frequency combinations and other satellites.

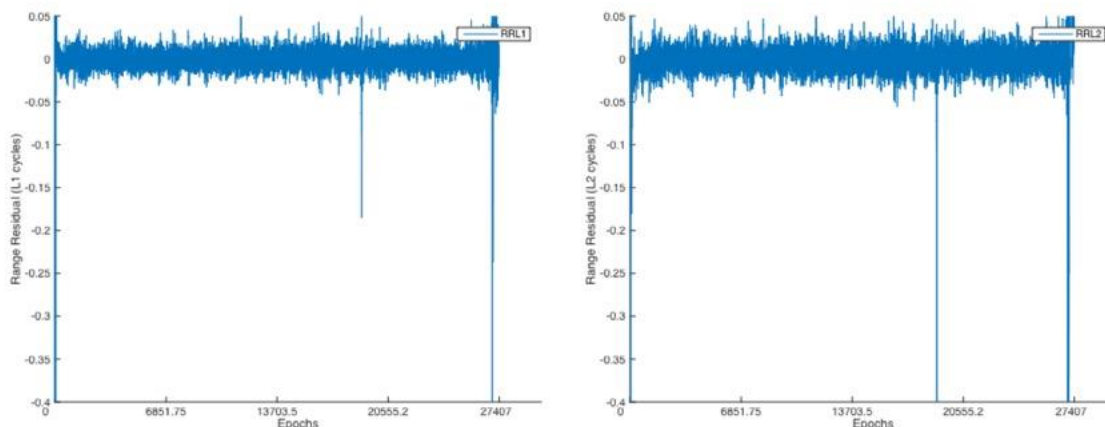
$$\delta IR = \left(\phi_a - \left(\frac{f_a}{f_b} \cdot \phi_b \right) \right)_{(i)} - \left(\phi_a - \left(\frac{f_a}{f_b} \cdot \phi_b \right) \right)_{(i-1)} \quad \text{Eq. 3}$$

3. RESULTS

3.1 Overview Results

The results presented in this paper are a subset of a much larger set.

Figure 1 illustrates the range residuals for GPS PRN32 (Block IIA satellite) and PRN14 (Block IIR satellite). The data were gathered for 27,400 epochs for PRN32 and 63,200 epochs for PRN14. The data for all the results in Figure 1 were gathered using a Leica GS10 GPS receiver, located at the University of Nottingham campus in Ningbo, China. It can be seen from these graphs that the Block IIR results are less noisy than those of the Block IIA satellite, illustrating an improvement in the pseudorange signal quality for a newer generation of GPS satellite.



Comparison of Triple Frequency GNSS Carrier Phase and Pseudorange noise using various satellite constellations. (9452)

Gethin Wyn Roberts (Faroe Islands), Craig Hancock and X Tang (China, PR)

FIG Congress 2018

Embracing our smart world where the continents connect: enhancing the geospatial maturity of societies
Istanbul, Turkey, May 6–11, 2018

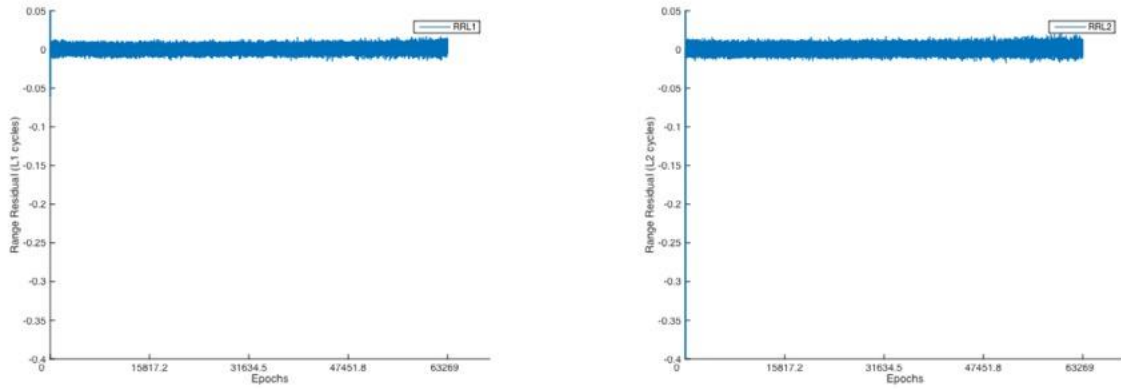


Figure 1, Range residual results (top) GPS PRN32 (Block IIA satellite) and (bottom) GPS PRN14 (Block IIR satellite).

Further to this, Figure 2 illustrates the corresponding L1L2 ionospheric residual plots for PRN32 and PRN14. Again, here it can be seen that the noise values for the block IIR satellite are less than those for the Block IIA satellite. Again, this implies a relative improvement in the quality of the carrier phase observable for the newer generation of GPS satellite.

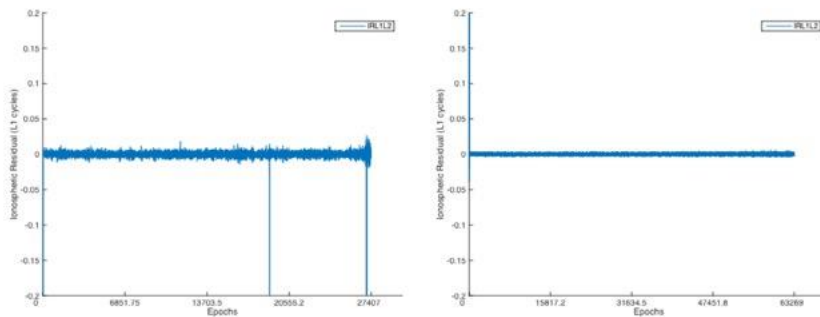


Figure 2, Ionospheric Residual results for the L1 and L2 combination (left) PRN32 (Block IIA) and (right) PRN14 (Block IIR).

If we compare BeiDou ionospheric residual results, this time through using a ComNav GNSS receiver, we can see the comparison of noise on the three ionospheric residual combinations, B1B2, B1B3 and B2B3, as well as the results from the three types of satellite orbits, ie MEO, IGSO and GEO. Figure 3 illustrates the ionospheric residual results for PRN07 (IGSO) for the three frequency combinations.

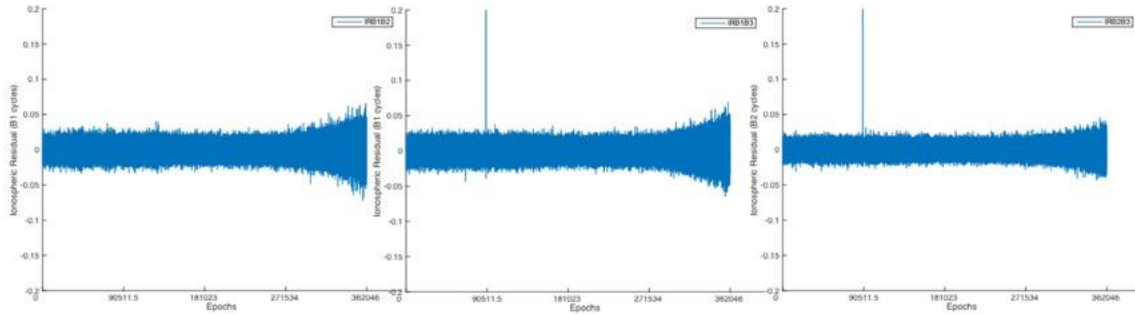


Figure 3, Ionospheric Residual results for BeiDou PRN07 (IGSO) for combinations B1B2 (left), B1B3 (centre), B2B3 (right).

Figure 4 illustrates the ionospheric residual results for PRN01 (GEO) for the three frequency combinations.

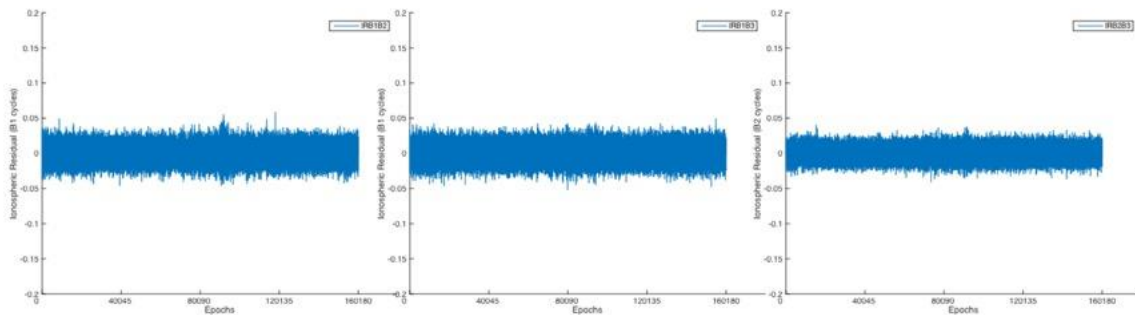


Figure 4, Ionospheric Residual results for BeiDou PRN01 (GEO) for combinations B1B2 (left), B1B3 (centre), B2B3 (right).

Figure 5 illustrates the ionospheric residual results for PRN12 (MEO) for the three frequency combinations.

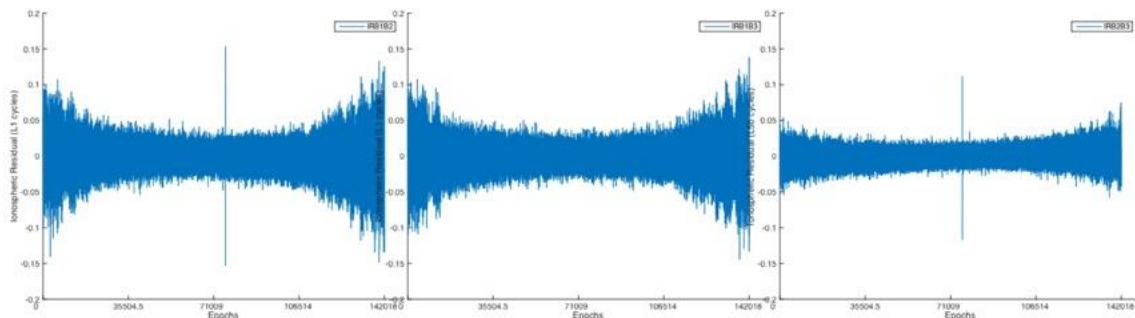


Figure 5, Ionospheric Residual results for BeiDou PRN12 (MEO) for combinations B1B2 (left), B1B3 (centre), B2B3 (right).

Here it can be seen that the B2B3 combination is generally less noisy than the B1B2 and B1B3. In addition to this, it can be seen that when the MEO and IGSO satellites are at lower elevation angles, the observables also become noisier. The GEO satellites have a constant elevation angle, and do not experience this phenomenon.

3.2 Detailed Results

This section presents results gathered on a single GNSS receiver located at the University of Curtin's GNSS research centre. The GNSS receiver used is a Trimble NET9, and the antenna used is a Trimble TRM 59800.00 SCIS choke ring antenna. The data was downloaded in BINEX format and converted into RINEX 3.02 format using RTKLIB [Takasu, 2013] software. Software was developed by the authors in Matlab in order to interrogate the data files and implement the range residual and ionospheric residual algorithms. RINEX 3.02 format was chosen due to its compatibility with multi-GNSS and multi-frequencies.

Results are presented for both Ionospheric residual and range residual results for various GNSS. The results presented have been calculated with varying elevation mask angles, ranging from 0° to 55° at 5° intervals. The RMS values of the resulting ionospheric residuals and range residuals were calculated and plotted against the respective elevation mask angle for each satellite and frequency combinations. This illustrates the influence of the elevation mask angle used on the results.

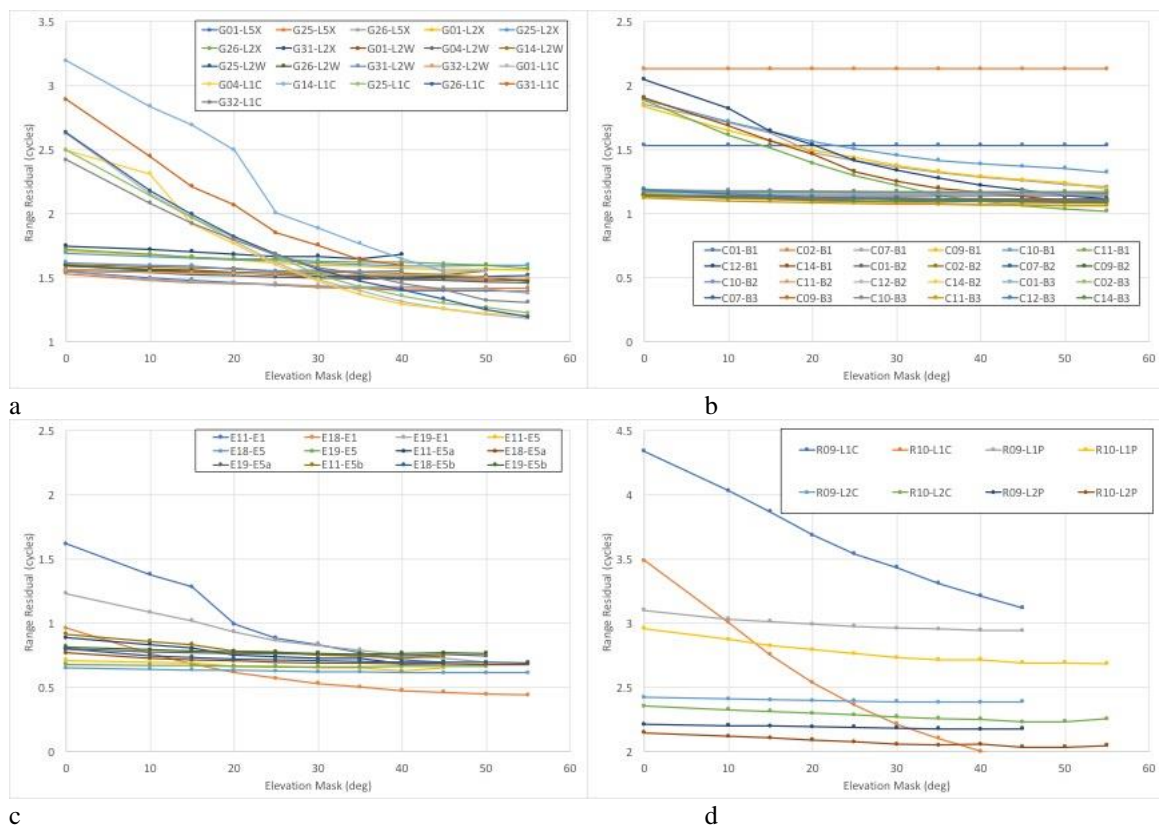
Typically, tens of thousands of epochs of data were used for every plotted point in the following figures. Further to this, not only are the results for the various frequencies and frequency combinations for the various GNSS illustrated, but also the various satellite types, MEO, GEO and IGSO, and various satellite Blocks for GNSS. GPS Block IIA (PRN04), Block IIR (PRN14), Block IIRM (PRN31) and Block IIF (PRN01, PRN26, PRN25 and PRN32) data were all analysed. Thus, the comparison of the various frequencies within each satellite system are illustrated, as well as the variations by comparing the various satellite constellation types and the various generations of GPS satellites. The BeiDou data illustrated are MEO (C12, C14, C11), IGSO (C09, C10, C07) and GEO (C01, C02). The data used were gathered on the 1st September 2015 in order to include the last remaining GPS Block IIA satellite (PRN04), which was taken out of operation on the 3 November 2015.

Figure 6 illustrates the range residual results for GPS (a), BeiDou (b), Galileo (c), GLONASS (d) and QZSS (e) respectively. These figures have been drawn so that the y-axis ranges are the same for each, hence illustrating the relative values.

Figure 6 (a) illustrates the range residual results for GPS. It can be seen that the L1 CA code results are the noisiest, with PRN14 being the noisiest, followed by PRN31, PRN04, PRN26, PRN01, PRN25 and PRN32. It can also be seen with these results that lower elevation angle mask increases the noise level. Both the L2 and L3 code results are less noisy. Looking at the detail, the L5 code results is less noisy than the L2 and affected less than the L1 results by

the changes in elevation mask angles used. Interestingly enough, the data file includes both the L2Y code and L2C code results. L2C only exists on the Block IIR and Block IIF satellites. The L2C code results are generally noisier than the L2Y code.

Figure 6(b) illustrates the results for the range residuals for the BeiDou satellites. Here it can be seen that the B1 code is affected more by low elevation mask angles, and hence multipath, than B2 and B3. It can also be seen that both the geostationary satellites' B1 results stand out, with satellite C02 being noisier than C01. The B2 and B3 values for both these GEO satellites are bunched up with the majority of the other results towards the middle of the figure. The pairs of B2 and B3 results for the Geo satellites are close to each other in values, and the pairs of B2 and B3 results for the other satellites are also close to each other. It can also be seen that the range residual results for BeiDou are generally lower than GPS, in units of cycles. Similarly, for Galileo Figure 6(c), the E1 results are worst, and affected more by low elevation masks, and hence multipath. Again, generally the Galileo results are seen to be improved over GPS. The GLONASS results, Figure 6(d) illustrate that the L1C results are generally noisier, and then the L1P, followed by L2C and L2P. PRN09 is also consistently generally noisier than PRN10. Finally, Figure 6(e) illustrates the results for QZSS. Again, L1C is the noisiest and affected most by low elevation mask angles.

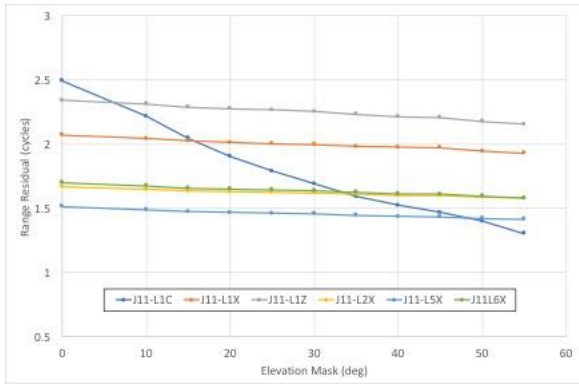


Comparison of Triple Frequency GNSS Carrier Phase and Pseudorange noise using various satellite constellations. (9452)

Gethin Wyn Roberts (Faroe Islands), Craig Hancock and X Tang (China, PR)

FIG Congress 2018

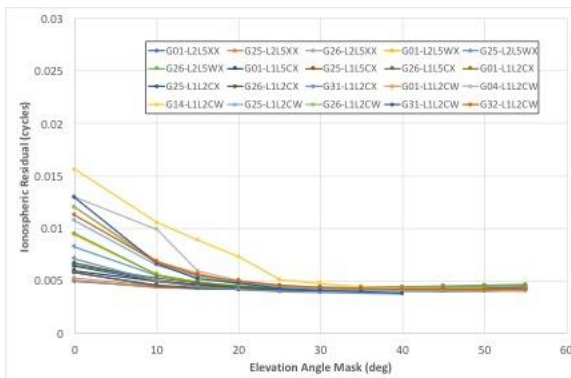
Embracing our smart world where the continents connect: enhancing the geospatial maturity of societies
 Istanbul, Turkey, May 6–11, 2018



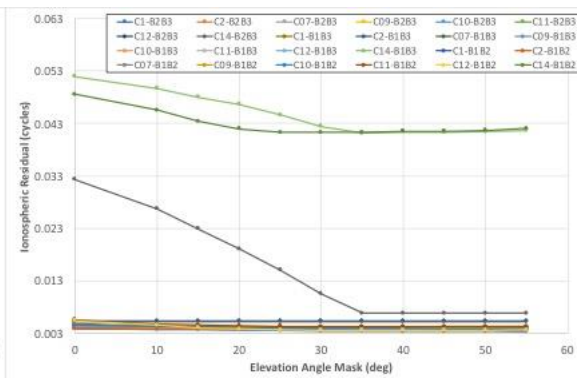
e

Figure 6, Range Residual results for GPS (a), BeiDou (b), Galileo (c), GLONASS (d) and QZSS (e).

Figure 7 illustrates the ionospheric residual results for the same satellites as Figure 6. This time, however, the resulting ionospheric residual values are calculated using pairs of data from the same satellite on different carrier frequencies. The range residual results compare the code and carrier from specific satellites and frequencies. Figure 7(a) shows that the ionospheric residual results are affected by low elevation masks, and that the L1L2CW (L1 CA code and L2 Y code available on all the satellites) combinations are the noisiest, followed by L2L5WX (L1 P code and L5 code available on Block IIF satellites, PRN 26, PRN01, PRN25), followed by L1L2CX (L1 CA code and L2 C code available on Block IIF and Block IIRM satellites, PRN31, PRN26, PRN01 and PRN25), followed by L1L5CX (L1C code and L5 code, Block IIF satellites, PRN01, PRN25, PRN26) and finally the least noisy were the L2L5XX results (L2 C code and L5 code available on Block IIF satellites, PRN26, PRN25 and PRN01). It can be seen that Block IIF satellite PRN32 has no L5 data, or L2 C code data.



a



b

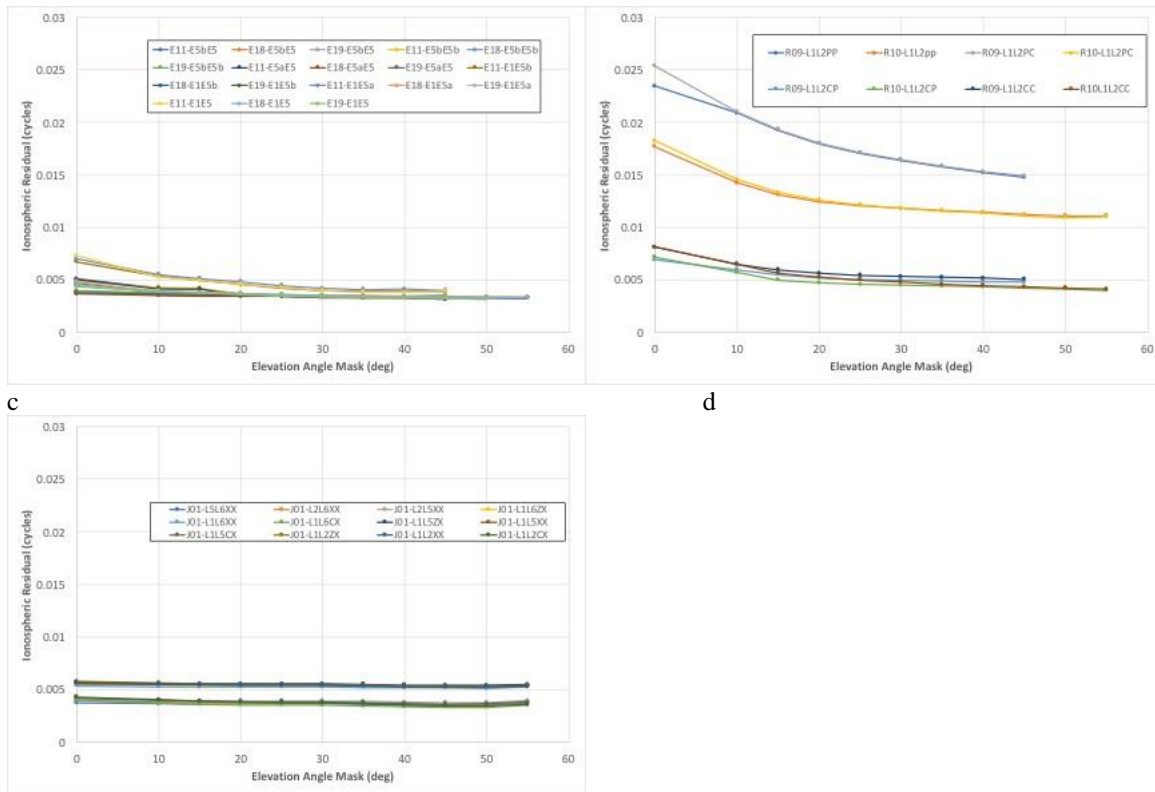
Comparison of Triple Frequency GNSS Carrier Phase and Pseudorange noise using various satellite constellations. (9452)

Gethin Wyn Roberts (Faroe Islands), Craig Hancock and X Tang (China, PR)

FIG Congress 2018

Embracing our smart world where the continents connect: enhancing the geospatial maturity of societies

Istanbul, Turkey, May 6–11, 2018



e
 Figure 7, Ionospheric Residual results for GPS (a), BeiDou (b), Galileo (c), GLONASS (d) and QZSS (e).

Figure 7(b) illustrates the BeiDou ionospheric residual plots, illustrating that satellite C14 is much noisier for all three combinations of B1B3, BB1B2 and B2B3 in that order. The B1B2 combinations for the satellites are generally the noisiest, and then the B1B3 and B2B3 combinations are intertwined. The Galileo results again illustrate that the E1 combinations are generally noisier, and again we see the effect of low elevation angle masks introducing more multipath noise, Figure 7(c). Generally, however, the Galileo results are less noisy than GPS, as are the BeiDou results.

The GLONASS results are again generally the noisiest, and again PRN09 is noisier than PRN10, with the L1P combinations being noisier, Figure 7(d). Figure 7(e) shows that there are generally two groups of results. The upper set consists of L1L2ZX, L1L5ZX, L1L2XX, L1L5XX, L1L6ZX and L1L6XX from highest to lowest noise respectively. The lower, less noisy, group consists of L1L2CX, L1L5CX, L2L5XX, L2L6XX, L1L6CX, and L5L6XX from highest to lowest noise respectively. Further details about the various codes and carrier values can be found in the RINEX 3.02 manual produced by the IGS [IGS, 2013].

CONCLUSIONS

These preliminary results illustrate that there are differences in the noise values for various GNSS, frequencies as well as satellite generations. It can be seen that generally L1, B1 and E1 have noisier results, and are affected more so by low elevation mask data, and hence multipath. It can also be seen that newer generations of satellites do indeed produce better quality data. Some specific satellites produce lower quality data such as GLONASS PRN09 and BeiDou C14. This could be due to multipath produced at the satellite.

REFERENCES

Goad, C., (1986). Precise Positioning with the GPS. Proceedings of the CERN Accelerator School of Particle Acceleration, CERN, Geneva.

IGS, RINEX The Receiver Independent Exchange Format Version 3.02, International GNSS Service (IGS), RINEX Working Group and Radio Technical Commission for Maritime Services Special Committee 104 (RTCM-SC104), April 3, 2013.

Roberts, G. W., (1997). Real Time On The Fly Kinematic GPS. PhD Thesis, the University of Nottingham.

Roberts, G. W.; Triple Frequency multi-GNSS Cycle Slip Detection using Ionospheric Residuals. FIG Working Week, Helsinki, Finland. 28 May – 2 June 2017.

Takasu. T. “Rtklib ver. 2.4.2 manual. http://www.rtklib.com/prog/manual_2.4.2.pdf,” Tech, 2013.

ACKNOWLEDGEMENTS

The work in this paper is supported by the Ningbo Science and Technology Bureau as part of the project ‘Structural Health Monitoring of Infrastructure in the Logistics Cycle (2014A35008)’, as well as the Young Scientist programme of Natural Science Foundation of China (NSFC) with a project code 41704024. The GNSS data used for this paper were obtained from the Curtin GNSS Research Centre’s at Curtin University <http://saegnss2.curtin.edu.au/ldc/>.

Comparison of Triple Frequency GNSS Carrier Phase and Pseudorange noise using various satellite constellations. (9452)

Gethin Wyn Roberts (Faroe Islands), Craig Hancock and X Tang (China, PR)

FIG Congress 2018

Embracing our smart world where the continents connect: enhancing the geospatial maturity of societies
Istanbul, Turkey, May 6–11, 2018

BIOGRAPHICAL NOTES

Gethin Wyn Roberts is an Associate Professor at Fróðskaparsetur (University of the Faroe Islands). He has authored and coauthored over 200 papers and been the investigator on UK and international research grants. He is past Chairman of the FIG's Commission 6, Engineering Surveys, and previously held posts at the University of Nottingham both in the UK and in China. He is a Fellow of the Chartered Institution of Civil Engineering Surveyors, and the Higher Education Academy. He holds a BEng in Mining Engineering and a PhD in Engineering Surveying and Geodesy both from the University of Nottingham, UK.

Craig M. Hancock is an Associate Professor in Geodesy and Surveying Engineering and the Head of Department of Civil Engineering at the University of Nottingham Ningbo China as well as the Head of the Geospatial and Geohazards Research Group. His current research interests include positioning in difficult environments and mitigation of GNSS errors.

Xu Tang is Research fellow in University of Nottingham Ningbo China. His interest is GNSS data processing for the huge structure deflection detection, PPP-RTK and GNSS clock correction estimation and analysis.

CONTACTS

Dr Gethin Wyn Roberts
Fróðskaparsetur
Tórshavn
FAROE ISLANDS
Tel. +298 292561
Email: gethinr@setur.fo
Web site: www.setur.fo

Comparison of Triple Frequency GNSS Carrier Phase and Pseudorange noise using various satellite constellations.
(9452)

Gethin Wyn Roberts (Faroe Islands), Craig Hancock and X Tang (China, PR)

FIG Congress 2018

Embracing our smart world where the continents connect: enhancing the geospatial maturity of societies
Istanbul, Turkey, May 6–11, 2018